Short Papers

Data Reduction Method for Q Measurements of Strip-Line Resonators

S. Toncich and R. E. Collin

Abstract—**This paper describes a technique that enables the attenuation constant α of a microstrip line to be found from the measured return loss curve as a function of frequency for a half wavelength resonator. Data averaging is incorporated and the effects of dispersion are included. This method does not require the use of an equivalent resonator model for the stripline, nor does it rely on graphical techniques.**

I. Introduction

A common technique used to determine the attenuation constant of a microstrip line is based on Q factor measurements made on resonators which are capacitively coupled via a small gap to a main line. Several techniques have been described in the literature for calculating the unloaded Q of these resonators from measured input reflection coefficient data [1]–[3]. These rely on graphical techniques developed by Ginzton [4] for measurements made on resonant cavities and are based on equivalent circuit models for the resonator. While these give good results for the high Q's (> 10 000) typically realizable for cavity resonators, the approximations are not always valid for the low Q's (200 or less) typical of microstrip resonators.

The usual expression for Q used in these techniques relates the propagation constant β, and the attenuation constant α, as follows

$$Q = \beta/2\alpha \tag{1}$$

where $\beta = (\omega/c)\sqrt{\epsilon_{\text{eff}}}$, $\omega = 2\pi f$, c is the speed of light, and ϵ_{eff} is the effective dielectric constant of the substrate. However, (1) does not include the effect of dispersion. For a dispersive line ϵ_{eff} becomes a function of frequency and the proper expression for Q becomes

$$Q = \frac{\omega \dfrac{d\beta}{d\omega}}{2\alpha} \tag{2}$$

where $\beta = (\omega/c)\sqrt{\epsilon_{\text{eff}}(f)}$. Therefore, the correct solution to the problem of determining the Q of a possibly dispersive line requires that measurements be made at several frequencies around the desired operating frequency, on several resonators of appropriate length, or some model must be included to account for dispersion as a function of microstrip geometry and frequency.

Along with accounting for dispersion, the detuning effect of fringing fields at the open end of the resonator must be included. For an open circuit resonator, this may be modeled as a fringing capacitance, or equivalently as an increase in electrical length of the resonator. The numerical value of the detuning capacitance may be determined by measurements made on two resonators, one twice the length of the other, or it can be found from curves available in the published literature [5].

This paper presents a technique that allows the attenuation constant to be found from a measured curve of $|\Gamma_{in}|^2$ versus frequency. Data averaging is incorporated and the effects of dispersion are included. The method does not rely on an equivalent resonator model. The salient features of this method are: 1) The Q and attenuation constant are solved for from averaged measured values for the input reflection coefficient for a given resonator. This is possible since all the required information is contained in a plot of $|\Gamma_{in}|^2$ versus frequency. To reduce the effect of measurement error on the data, a curve fitting technique is used to find the best quadratic curve to fit the data points, that are chosen symmetric about the measured minimum value of Γ_{in}. Since the measured minimum may not be the actual minimum, the minimum is found from the quadratic curve fit to the data. Once the actual minimum is found, seven points (three above and three below) chosen symmetrically around this minimum are chosen to calculate the attenuation constant at resonance. A quadratic polynomial is sufficient to represent the $|\Gamma_{in}|^2$ curve near resonance for data points up to ±10% from the measured resonant frequency. 2) An analytic expression for dispersion, developed by Getzinger [6] may be used to describe the variation in phase around the resonance point,

$$\epsilon_{\text{eff}}(f) = \epsilon_r - \frac{\epsilon_r - \epsilon_{\text{eff}}}{1 + G(f/f_p)^2} \tag{3}$$

where $f_p = Z_c/8\pi h$, $G = 0.6 + 0.009Z_c$, ϵ_{eff} is the zero frequency effective dielectric constant, h is the substrate height in cm, and f and f_p are in units of GHz. (See Fig. 1).

A more accurate formula for the dispersion has been given by Kobayashi [7], and could be used in place of (3) for greater accuracy.

For a half wavelength resonator at resonance, the phase shift for Γ_{in} is -2π radians. This fact, along with a dispersion model for β allows one to calculate the phase shift due to the coupling network for resonance, if some estimate is available on the fringing capacitance at the open end. At resonance, the total phase shift is given by

$$-2n\pi = \theta_{11}(f_r) - 2\beta(f_r)l - 2\theta_{oc}(f_r) \tag{4}$$

where $\theta_{11}(f)$ is the contribution due to the coupling network, $\theta_{oc}(f)$ is the contribution from the open end, l is the resonator length. For a half wave length resonator, $l = \lambda_g/2$ and $n = 1$.

A small gap may be modeled as a capacitive *pi* network, therefore an analytic expression for $\theta_{11}(f)$ may be employed near resonance [8]. This expression will be developed later. Calculating $\theta_{11}(f_r)$ by (4) also serves to remove any phase error or offset introduced by a poor choice of reference plane when making the measurement. The fringing capacitance was determined from published data [5], and is a function of microstrip geometry.

This technique was implemented as a computer program and used to analyze several sets of resonator data. The results are presented at the end of this paper.

Manuscript received January 22, 1991; revised February 4, 1992. This work was supported by NASA Lewis Research Center under Grant NC3-29.

S. Toncich and R. E. Collin are with the Electrical Engineering and Applied Physics Department, Case Western Reserve University, Cleveland, OH 44106.

IEEE Log Number 9201724.

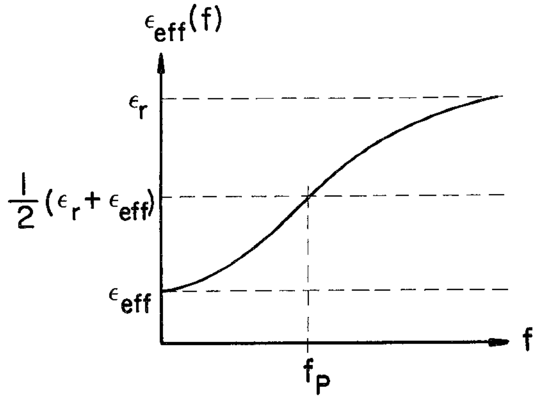

Fig. 1. Dispersion characteristics of effective dielectric constant for a microstrip line.

II. Theory

The attenuation constant for a given microstrip geometry at a given frequency can be determined from measurements made on capacitivly coupled half wave resonators. From the measurements of input reflection coefficient one can extract all the desired information without resorting to the use of a lumped parameter equivalent circuit for the resonator, as shown in Fig. 2. The coupling network can be represented as a symmetrical capacitive pi network, whose S parameters are given by

$$S_{11} = S_{22} = \frac{Y_c^2 + \omega^2(2C_1C_2 + C_1^2)}{Y_c^2 - \omega^2(2C_1C_2 + C_1^2) + 2j\omega(C_1 + C_2)Y_c}$$

$$\rho_{11} = |S_{11}| \tag{5}$$

$$= \frac{Y_c^2 + \omega^2(2C_1C_2 + C_1^2)}{\{[Y_c^2 - \omega^2(2C_1C_2 + C_1^2)]^2 + 4\omega^2(C_1 + C_2)^2Y_c^2\}^{1/2}} \tag{6}$$

$$\arg(S_{11}) = \theta_{11} = -\tan^{-1}\frac{2\omega(C_1 + C_2)Y_c}{Y_c^2 - \omega^2(2C_1C_2 + C_1^2)} \tag{7}$$

$$S_{12} = S_{21} = (1 - \rho_{11}^2)^{1/2} \exp j(\theta_{11} \pm \pi/2). \tag{8}$$

It is not necessary to express the coupling network S parameters in terms of the capacitances in the equivalent network. The formulas developed later depend only on the requirement that the coupling network is symmetrical and lossless, i.e. $S_{11} = S_{22}$.

To account for the fringing capacitance C_f at the open circuit end, we can write

$$\Gamma_{oc} = \exp(-j2\theta_f) \tag{9}$$

where

$$\theta_f = \tan^{-1}(\omega C_f/Y_c). \tag{10}$$

The effect of the fringing capacitance is to increase the effective electrical length of the line and is seen as a detuning effect. The value of C_f is a function of the line width as well as substrate dielectric constant and thickness. Numerical values for C_f may be found in the literature, or θ_f may be measured using lines of different physical lengths [5].

At the coupling network, Γ_L for the resonator may be written as

$$\Gamma_L = \Gamma_{oc}\exp(-2j\beta l - 2\alpha l) = \rho_L \exp(-2j\beta l - 2j\theta_f) \tag{11}$$

where $\rho_L = \exp(-2\alpha l)$ and α is the attenuation constant. If radiation is present $|\Gamma_{oc}| < 1$, and will result in a reduced value of ρ_L, which can not be separated from the ρ_L due to attenuation in the conductor and dielectric, unless measurements are made on lines

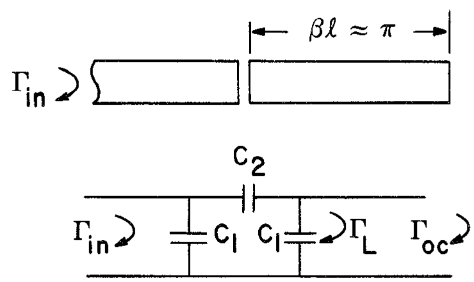

Fig. 2. Equivalent circuit for a gap coupled resonator.

of different lengths. If ρ_{L1} and ρ_{L2} are found for two resonators of length l_1 and l_2 respectively, then

$$\alpha = \frac{1}{2(l_2 - l_1)}\ln\left(\frac{\rho_{L1}}{\rho_{L2}}\right).$$

The input reflection coefficient Γ_{in} is given by

$$\Gamma_{in} = S_{11} + \frac{S_{12}^2\Gamma_L}{1 - S_{11}\Gamma_L} = \frac{\rho_{11} - \rho_L e^{j\phi}}{1 - \rho_{11}\rho_L e^{j\phi}}\exp(j\theta_{11}) \tag{12}$$

where $\phi = \theta_{11} - 2\beta l - 2\theta_f$. From (12) we get

$$\rho_{in}^2 = |\Gamma_{in}|^2 = \frac{\rho_{11}^2 + \rho_L^2 - 2\rho_{11}\rho_L\cos\phi}{1 + \rho_{11}^2\rho_L^2 - 2\rho_{11}\rho_L\cos\phi} \tag{13}$$

and

$$\tan(\varphi - \theta_{11}) = \frac{\rho_L(\rho_{11}^2 - 1)\sin\phi}{\rho_{11}(1 + \rho_L^2) - \rho_L(1 + \rho_{11}^2)\cos\phi} \tag{14}$$

where $\arg(\Gamma_{in}) = \varphi$. The minimum value of ρ_{in} occurs for $\phi = -2n\pi$ and is given by

$$\rho_m^2 = \frac{(\rho_{11} - \rho_L)^2}{(1 - \rho_{11}\rho_L)^2} \tag{15}$$

and

$$\arg(\Gamma_{in,m}) = \begin{cases} \theta_{11}, & \rho_{11} > \rho_L \\ \theta_{11} \pm \pi, & \rho_{11} < \rho_L \end{cases} \tag{16}$$

From (15) it is seen that for critical coupling ($\rho_m = 0$), it is required that $\rho_{11} = \rho_L$. When $\rho_{11} < \rho_L$ the resonator is over coupled, for $\rho_{11} > \rho_L$ it is under coupled.

For a given microstrip geometry, gap spacing, and frequency range, the measured values corresponding to (12) are unique, and so the required attenuation constant can be solved for using (12) and (13).

For near critical coupling, (7) reduces to

$$\theta_{11} = -2\omega(C_1 + C_2)/Y_c = -2\omega Z_c C_T \tag{17}$$

where $Z_c = 1/Y_c$ is the characteristic impedance of the line. The angle $\theta_{11}(f_r)$ can be determined at the measured resonant frequency point of the resonator from

$$\phi = -2\pi = \theta_{11}(f_r) - 2\beta(f_r)l - 2\theta_f(f_r) \tag{18a}$$

which gives

$$\theta_{11}(f_r) = -2\pi + 2(f_r)l + 2\theta_f(f_r) \tag{18b}$$

where f_r is the resonant frequency of the coupled line. θ_f can be determined from (10) using published data, and θ_{11} can be determined from (18). Note that $f_r \neq f_o$, the design resonant frequency, so the difference between f_o and f_r represents the combined detuning effects due to the coupling network, fringing, and dispersion.

To solve (18), $\beta(f_r) = (\omega/c)\sqrt{\epsilon_{\rm eff}(f)}$ must be known. If no dispersion is present, $\epsilon_{\rm eff}(f) = \epsilon_{\rm eff}(0)$ and $\beta(f)$ is known. For dispersive lines, Getzinger's expression for the dielectric constant is used for the examples considered in this paper.

For a half wave length resonator

$$l = \lambda_g/2 = \frac{1}{2}\frac{\lambda_o}{\sqrt{\epsilon_{\rm eff}(f_o)}} = \frac{c}{2f_o\sqrt{\epsilon_{\rm eff}(f_o)}} \tag{19}$$

where f_o is the resonant frequency of the uncoupled line. Therefore, (18a) at resonance can be written as

$$\phi = -2n\pi = \theta_{11}(f_r) - 2\pi\frac{f_r}{f_o}\left[\frac{\epsilon_{\rm eff}(f_r)}{\epsilon_{\rm eff}(f_o)}\right]^{1/2} - 2\tan^{-1}(2\pi f_r Z_c C_f) \tag{20}$$

which may be used to solve for $\theta_{11}(f_r)$, the phase shift due to the coupling network at the resonance point.

Over a $\pm 5\%$ frequency range near reasonance, $\cos\phi$ in (13) may be replaced by $1 - \phi^2/2$ where ϕ now represents the phase change from $-2n\pi$. Let $B = \rho_{11}\rho_L$, then (15) becomes $(\rho_{11} - \rho_L)^2 = (1 - B)^2\rho_m^2$ and (13) becomes

$$\rho_{\rm in}^2 = \frac{(1-B)^2\rho_m^2 + \phi^2 B}{(1-B)^2 + \phi^2 B} \tag{21}$$

at resonance. In (21) ϕ now represents the change in $\theta_{11} - 2\beta l - 2\theta_f$ away from $-2n\pi$. We can write this as

$$\phi = (d\phi/df)(f - f_r) \quad \text{or}$$

$$\phi = \left[f_r\frac{d(\theta_{11} - 2\theta_f)}{df} - 2lf_r\frac{2\pi}{c}\frac{d}{df}(f\sqrt{\epsilon_{\rm eff}(f)})\right]\frac{f - f_r}{f_r} \tag{22}$$

Now

$$\frac{d}{df}(f\sqrt{\epsilon_{\rm eff}(f)} = \sqrt{\epsilon_{\rm eff}(f)} + f\frac{1}{2\sqrt{\epsilon_{\rm eff}(f)}}\frac{d\epsilon_{\rm eff}(f)}{df}$$

and using (3) gives

$$\frac{d}{df}(f\sqrt{\epsilon_{\rm eff}(f)}) = \sqrt{\epsilon_{\rm eff}(f)}\left(1 + \frac{A}{\epsilon_{\rm eff}(f)}\frac{\epsilon_r - \epsilon_{\rm eff}}{(1+A)^2}\right) \tag{23}$$

where $A = G(f/f_p)^2$. Since $\theta_f = \tan^{-1}(2\pi f Z_c C_f)$

$$\frac{d\theta_f}{df} = \frac{2\pi Z_c C_f}{1 + (2\pi f Z_c C_f)^2}. \tag{24}$$

For a typical coupling network, $\theta_{11}(f) = -2\omega Z_c C_T$ so

$$\frac{d\theta_{11}}{df} = -4\pi Z_c C_T. \tag{25}$$

Combining (23), (24), and (25) in (22) gives

$$\phi = -S\frac{\Delta f}{f_r} \tag{26a}$$

where

$$S = \theta_{11}(f_r) - \frac{4\pi Z_c f_r C_f}{1 + (2\pi f_r Z_c C_f)^2} - 2\pi\frac{f_r}{f_o}\left[\frac{\epsilon_{\rm eff}(f)}{\epsilon_{\rm eff}(f_o)}\right]^{1/2} \cdot \left(1 + \frac{A}{\epsilon_{\rm eff}(f_r)}\frac{\epsilon_r - \epsilon_{\rm eff}}{(1+A)^2}\right). \tag{26b}$$

The frequency sensitivity of the network is determined by the slope parameter S, which includes dispersion effects. If we now let $\phi = S\Delta f/f_r = S\delta$ where $\delta = \Delta f/f_r$, (21) becomes

$$\rho_{\rm in}^2 = \frac{\rho_m^2 + [S^2B/(1-B)^2]\,\delta^2}{1 + [S^2B/(1-B)^2]\,\delta^2} \tag{27}$$

where as before, $B = \rho_{11}\rho_L$. Since we have an expression for S, (27) may be solved for B by assuming that over a small range of frequencies, i.e., $\delta < 0.1$, $\rho_{11}\rho_L$ remains essentially constant, so that two values of $\rho_{\rm in}^2$, say $\rho_{\rm in1}^2$ and $\rho_{\rm in2}^2$ may be chosen, giving two equations for the unknowns, ρ_m and B.

If $\rho_{\rm in}^2$, ρ_m^2, and $W = S^2B/(1-B)^2$ were known to great precision near resonance, (27) could be solved accurately for ρ_L. However, since measured values of $\rho_{\rm in}^2$ are subject to random errors and round off by the measurement instrument, different sets of selected points will give different values for ρ_L. Since a 5% to 10% error is possible as a result of an experimental set-up, a modified approach is needed to smooth out the errors. Since a large number of data points are available near resonance, curve fitting may be employed to extrapolate $\rho_{\rm in}^2$ values back to resonance to get a more accurate value for ρ_m^2.

Since only data points near resonance are used, the expression for ϕ in (22) or S in (26) offers a valid, linear approximation to the phase change near resonance.

For measured pairs of values of $\rho_{\rm in}^2$, say ρ_1^2 and ρ_2^2 at δ_1 and δ_2, we can solve for ρ_m^2 and W to give

$$W = \frac{\rho_1^2 - \rho_2^2}{(1-\rho_1^2)\,\delta_1^2 - (1-\rho_2^2)\,\delta^2} \tag{28}$$

$$\rho_m^2 = \frac{\rho_2^2(1-\rho_1^2)\,\delta_1^2 - \rho_1^2(1-\rho_2^2)\,\delta_2^2}{(1-\rho_1^2)\,\delta_1^2 - (1-\rho_2^2)\,\delta_2^2} \tag{29}$$

If several pairs of points were used to calculate a number of values for ρ_m^2 and W, a least square polynomial fit can be used to extrapolate back to $f = f_r$ to give a good estimate on W and ρ_m^2 at $f = f_r$.

Since S is known and B can be solved for, ρ_L may be determined to be

$$\rho_L = \pm(1-B)\rho_M/2 + [(1-B)^2\rho_M^2/4 + B]^{1/2} \tag{30}$$

where ρ_M is the averaged value of ρ_m. The upper sign is used when $\rho_L > \rho_{11}$ and the lower sign when $\rho_L < \rho_{11}$. From ρ_L, we get

$$\alpha = -\frac{1}{2l}\ln\rho_L \tag{31}$$

If ρ_L is close to 1, ρ_L must be accurately known to avoid large errors in α.

Although these equations were solved for several sets of data points, only one calculation using the smoothed minimum value of $|\Gamma_{\rm in}|^2$ (i.e., ρ_M^2), and one value above and below it is really necessary. This is because the quadratic curve represents the "best fit" to the seven data points chosen so the computed minimum value is a weighted average which depends on six other points.

The technique of using a quadratic equation to represent $|\Gamma_{\rm in}|^2$ versus frequency is valid only for data points near the minimum value of $|\Gamma_{\rm in}|^2$, say within $\pm 10\%$. For points far from resonance, the quadratic approximation is not an accurate representation of the $|\Gamma|_{\rm in}^2$ curve. Smoothing the data by means of a least squares fit to the measured $\rho_{\rm in}^2$ versus frequency data allows us to use the above equations to obtain an accurate value for α.

III. Numerical Results and Conclusions

A program written to implement this technique was used to analyze several sets of resonator data. The resonators were constructed

TABLE I

Resonator	Design Resonant Frequency (GHz)	Actual Resonant Frequency (GHz)	Q	P_L
(1)	20.0	18.920	82	.9641
(2)	20.0	19.194	149	.9667
(3)	16.0	15.41	182	.9850
(4)	12.0	11.505	201	.9850
(5)	20.0	18.885	77	.9619
(6)	20.0	19.173	128	.9613
(7)	16.0	15.342	117	.9745
(8)	20.0	17.897	57	.9195
(9)	8.0	7.522	131	.9773
(10)	16.0	13.457	19	.8641
(11)	20.0	16.406	13	.8144

Resonators

Shielded Lines	
(1) #5S 10 mil Duroid	(6) #5L 10 mil Duroid
(2) #5L 10 mil Duroid	(7) #4S 10 mil Cuflon
(3) #4S 10 mil CuFlon	(8) #5L 31 mil CuFlon
(4) #3S 10 mil CuFlon (short shield)	(9) #2S 31 mil CuFlon
Unshielded Lines	(10) #4S 31 mil CuFlon*
(5) #5S 10 mil Duroid	(11) #5S mil Cuflon*

*Low Q caused by poor metallization in the fabrication process.

on Duroid ($\epsilon_r = 2.17$) and CuFlon ($\epsilon_r = 2.1$) substrates of thickness of 10 or 31 mils. The characteristic impedances of all lines was 50 Ω. Table I shows the results obtained for shielded and unshielded resonators, along with the design resonant frequency and calculated Q. The resonators were manufactured by a metalization process and the variation in measured Q for similar resonators is believed to be due to the quality of the metalization. The design and construction of the resonators was carried out at the NASA Lewis Research Center [10] as were the measurements.

The calculated Q's listed in this table are in good agreement with estimated Q's determined from the bandwidth of the $|\Gamma_{in}|^2$ curve at the 6 dB return loss points.

The approach presented here offers several advantages over other techniques commonly used to determine the Q of a microstrip resonator. They are:

1) ρ_L and Q are determined fom the fitted $|\Gamma_{in}|^2$ curve directly.

2) Using seven measured data points allows more of the available information to be used to determine the Q.

3) Curve fitting of the data reduces measurement induced error.

4) A dispersion model is introduced so that the effects of dispersion are included.

5) An accurately established reference plane is not required in making the measurements.

6) No detailed model of the coupling gap is needed. This approach is suitable for analyzing resonators using asymmetric coupling gaps, where $S_{11} \neq S_{22}$, with only slight modification.

References

[1] D. Kajfez and E Hwan, "Q-factor measurements with network analyzer," *IEEE Trans. Microwave Theory Tech.*, vol. 32, pp. 666–670, July 1984.

[2] A. Khanna and Y. Gerault, "Determination of loaded, unloaded, and external quality factors of a dielectric resonator coupled to a microstrip line," *IEEE Trans. Microwave Theory Tech.*, vol. 31, pp. 261–264, Mar. 1983.

[3] R. A. Pucel and D. J. Masse, "Losses in microstrip," *IEEE Trans. Microwave Theory Tech.*, vol. 16, pp. 348–350, June 1968.

[4] E. H. Ginzton, *Microwave Measurements.* New York: McGraw Hill, 1957, pp. 391–434.

[5] P. Silvester and P. Benedek, "Equivalent capacitance of microstrip open circuits," *IEEE Trans. Microwave Theory Tech.*, vol. MTT-20, pp. 511–516, Aug. 1972.

[6] W. J. Getsinger, "Microstrip dispersion model," *IEEE Trans. Microwave Theory Tech.*, vol. 21, pp. 34–39, Jan. 1973.

[7] M. Kobayashi, "A dispersion formula satisfying recent requirements in microstrip CAD," *IEEE Trans. Microwave Theory Tech.*, vol. 36, pp. 1246–1250, Aug. 1988.

[8] P. Benedek and P. Silvester, "Equivalent capacitance of microstrip gaps and steps," *IEEE Trans. Microwave Theory Tech.*, vol. 20, pp. 729–733, Nov. 1972.

[9] K. C. Gupta, R. Garg, and I. J. Bahl, *Microstrip Lines and Slotlines.* Dedham Mass.: Artech House, 1979, pp. 130–136.

[10] R. R. Romanofski, *et al.* "An experimental investigation of microstrip properties on soft substrates from 2 to 40 GHz," in *1985 IEEE MTT-S International Microwave Symposium Dig.*, St. Louis, MO, 1985, pp. 675–678.

Conformal Mapping Analyses of Microstrips with Circular and Elliptical Cross-Sections

M. A. Martens, R. W. Brown, and E. M. Haacke

***Abstract*—A new conformal transformation is derived in terms of a Schwarz-Christoffel transformation involving elliptic integrals of the first and third kind. This mapping function is used to give exact solutions for TEM excitations of microstrips and coupled microstrips with circular and elliptical cross-sections. Using these maps, the uniformity of the TEM mode magnetic field inside an elliptical slotted tube transmission line is investigated.**

I. Introduction

Due to the interest in nonplanar microstriplines with circular and elliptical cross-sections [1]–[7] it is certainly useful if one can find an analytic solution for the fields produced in these geometries. Some of the methods suggested in the literature involve either infinite series [1], [3], [7] or iterations [5]. In contrast to these methods, the conformal mapping technique, if successful, provides an exact closed-form solution. Although conformal mapping has been applied to this class of problems [2], [4], [6], the geometries are mapped into a finite region of a domain where the conductors are planar and then one or more of the transverse dimensions of the conductors are assumed to extend to infinity.

It is the purpose of this paper to present a complete set of conformal transformations that are used to analyze the TEM modes of the circular and elliptical geometries shown in Fig. 1. No assump-

Manuscript received June 18, 1991; revised February 7, 1992. This work was supported by the Whitaker Foundation and by Picker International.

M. A. Martens was with the Department of Physics, Case Western Reserve University, Cleveland, OH 44106. He is presently with Fermi National Accelerator Laboratory, Batavia, IL 60510.

R. W. Brown is with the Department of Physics, Case Western Reserve University, Cleveland, OH 44106.

E. M. Haacke is with the Department of Physics, Case Western University, Cleveland, OH 44106. He is also with the Radiology Department, University Hospitals of Cleveland.

IEEE Log Number 9201725.